Span Order Dependency for Nonlinear Interference Noise over In-homogeneous Multispan O-band Coherent Transmission

Daniel J. Elson,[1,*] Mindaugas Jarmolovičius,[2] Noboru Yoshikane,[1] Takehiro Tsuritani,[1] Eric Sillekens,[2] Polina Bayvel,[2] Robert Killey,[2] and Yuta Wakayama[1]

[1] *KDDI Research, Inc., 2-1-15 Ohara, Fujimino 356-8502, Japan*
[2] *Optical Networks Group, UCL (University College London), London*
**xda-elson@kddi.com*

Abstract: Coherent O-band transmission was conducted in the nonlinear regime. For spans with an in-homogeneous zero dispersion wavelength, the amount and spectral content of non-linear interference noise was found to be dependent on span order.

1. Introduction

A consistent growth of data traffic inside data centers driven by global cloud services continues to push the bandwidth requirements of data centre interconnects (DCI)s. Coherent pluggable transceivers are becoming a mature technology for use in DCIs with dense wavelength division multiplexed links [1], and the O-band is being considered a candidate for a new 800G-LR1 standard [2]. DCI are typically limited to <40 km but reach extension can be performed with only a simple single-stage bismuth-doped fibre amplifier (BDFA) [3]. Interest in coherent O-band transceivers has grown because their operation in the near-zero dispersion window helps to improve energy efficiency as the dispersion compensation step in the digital signal processing (DSP) chain can be avoided [4]. In addition, transmission in O-band allows a single doped amplifier to provide gain over ultra-wide bandwidths, even larger than that of a C+L system [5]. This mitigates the higher attenuation in the O-band, compared to multiband systems. Furthermore, the ultrawideband operation can support the higher throughput and port number requirements for the next generation DCIs, where the aggregate bandwidth [6] is more important than spectral efficiency. In such ultrawideband or repeatered systems, the resultant nonlinear noise (NLIN) can become a factor and concern remains about impact of four wave mixing (FWM) near zero dispersion [7]. Previously, we demonstrated NLIN can be suppressed by managing the launch power at each span [4]. However, NLIN generation and its power have not been characterised comprehensively. In this paper we investigate the amount of NLIN generated around the zero dispersion wavelength in G.657.A1 fibres from three different manufacturers.

2. O-band transmission over multiple deployed fibre-optic spans.

Figure 1 shows the experimental setup for O-band transmission. The characteristics of the BDFA's were measured previously in [3]. The transmitter consisted of a centre test channel and two adjacent dummy test channels. The channels were generated from three external cavity lasers (ECLs) in an odd-even pattern spaced at 50 GHz, and were tuned to a 200 GHz grid. The grid started at 1283 nm and finished at 1336.8 nm resulting in 48 channels. The three test channels in the back-to-back configuration centred at 1300 nm are shown in Fig. 2b. The centre and adjacent channels were modulated by separate single polarisation IQ modulators at 40 GBd with Nyquist filtered 16-QAM signals (roll off 0.01) generated by a 120-GSa/s arbitrary waveform generator (AWG). Each set of test channels were polarisation multiplexed (PM) by creating a copy and recombining after a fibre delay. The lengths of fibre for the centre and adjacent channels were approximately 5 m and 10 m, respectively, to decorrelate polarisations. After PM emulation (PME) the signals were amplified with a BDFA and coupled together ready for transmission. The transmission spans were configured from installed fibre cables, which accommodated 200 fibres of G.657.A1 in 12-mm diameter cables [3]. The attenuation α and CD profiles of the spans were characterised and are shown in Fig. 2a. The launch power into each span was controlled by a VOA set to launch +6 dBm per channel over a total transmission distance of 90 km. Span A, B and C had a zero dispersion wavelengths (λ_A, λ_B and λ_C) of 1314.1 nm, 1314.0 nm and 1307.9 nm, respectively. Two spans were connected in different orders to measure the effects of λ_0 on nonlinear noise generation. Three configurations were experimentally tested: A followed by C (A→C), C followed by A (C→A) and A followed by B (A→B).

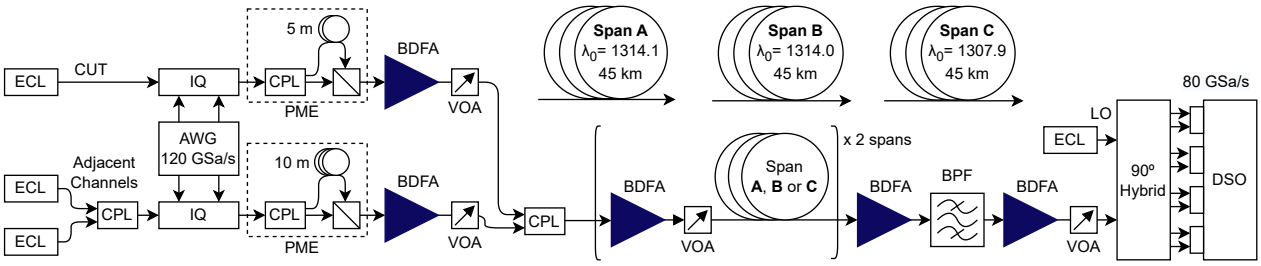

Fig. 1: Setup showing transmitter, installed fibre spans and coherent receiver

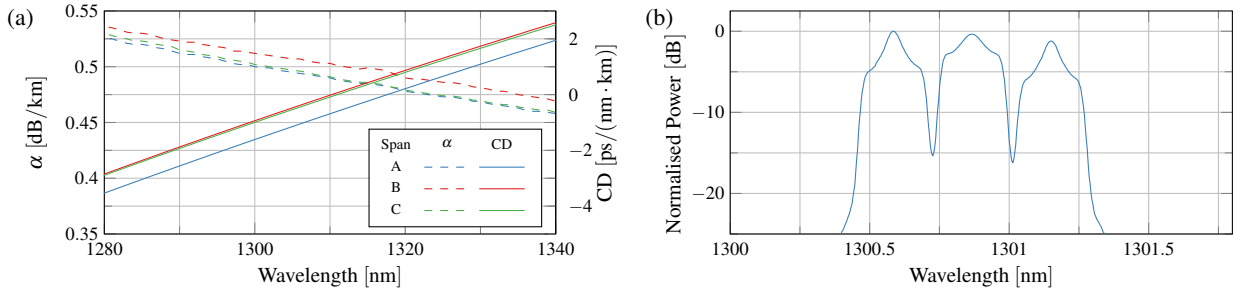

Fig. 2: (a) Fibre attenuation α and chromatic dispersion CD as a function of wavelength for each span, (b) close up of 50 GHz-spaced transmitted signals centred at 1300.7 nm

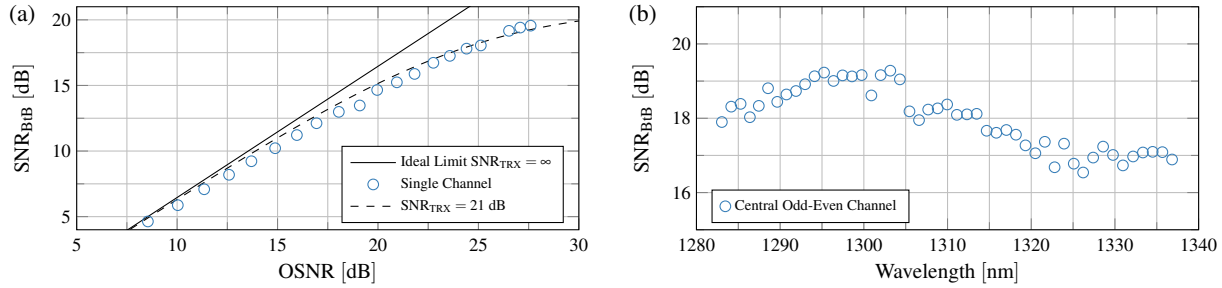

Fig. 3: Back-to-back performance measurements (a) SNR vs OSNR for just the central channel at 1300 nm (b) SNR of the central channel after combining with even channels as a function of wavelength

After transmission the signals were amplified and bandpass filtered with a width of 1.1 nm centred on the CUT. The signal was then filtered, amplified to maintain a fixed input power of 6 dBm into the receiver. The electrical signals were digitised at a fixed sample rate of 80 GSa/s and processed offline. First, frequency offset removal was performed before being downsampled to 2 samples per symbol for root raised cosine filtering. Subsequently, a radially directed equaliser was used to recover the distorted signal. The signal was downsampled to 1 sample per symbol for carrier recovery and, finally, IQ orthogonalisation before calculation of signal-to-noise ratio (SNR). In addition, we use split-step Fourier method (SSFM) simulations to compare with our measurements. The SSFM simulations were implemented using the local-error method [8] with small goal error of $\delta_G = 10^{-9}$ to ensure large number of steps and prevent overestimation of FWM. The simulations used measured fibre characteristics and assumed $\gamma = 2$ W^{-1}km^{-1} [9]. Each channel was simulated with 2^{16} symbol sequence which was sufficient as there were no visible NLI artefacts in the results.

3. Results and discussion

Figure 3a shows the measured SNR in the back-to-back setup for the central channel only, bypassing the transmission spans and turning off the adjacent channels. The wavelength was the channel under test (CUT) was set to 1300 nm and then amplified spontaneous emission noise (ASE) was added, to reduce the received optical SNR (OSNR). The solid line represents the theoretical limit in case of the transceiver SNR of SNR$_{TRX} = \infty$ and the dashed line - the limit for a transceiver with a maximum SNR of 21 dB. The adjacent channels were then added, restoring the odd-even configuration and SNR was measured as a function of wavelength as shown in Figure 3b. Here, the wavelength dependency of the transceiver can be seen. The maximum SNR was then limited to 19.3 dB at around 1300 nm and slowly dropped to around 17 dB around 1330 nm.

A transmission experiment over two spans was then simulated and performed. The order of the spans was set to AB, AC and CA and the SNR of the CUT was measured. This is shown in Fig. 4. The zero dispersion wavelengths of the transmission spans A, B and C are also shown. The SNR dips for a specific wavelength for each configuration. For the A→B configuration the minimum expected SNR for occurs at 1315.4 nm coinciding with the experimental measurement and the fibre zero dispersion wavelength was 1314.0 nm. There was consistently an offset between maximum nonlinear noise generation and zero dispersion wavelength. It is expected that FWM would be the dominant source of NLIN near zero dispersion [9]. It has been shown previously that FWM efficiency is asymmetric around the [10] pump wavelength when centered on the zero dispersion. Since there is better FWM efficiency for frequencies lower than pump frequency, longer wavelengths would expect higher NLIN. Additionally, it has also been demonstrated the comb line generation through FWM in the negative dispersion is less efficient [11] hence, more NLIN at wavelengths longer than the zero dispersion wavelength should be expected.

The configuration was then changed to A→C, where the average zero dispersion wavelength was 1311.0 nm. The minimum SNR shifted towards the average zero dispersion wavelength but remained offset by 3.5 nm. The span order was then reversed C→A. Here, the average zero dispersion wavelength remains the same but the minimum SNR shifted even further towards the shorter wavelengths (1310.4 nm). The experiment shows the same trend, where the minimum SNR was at 1311.1 nm. This demonstrates that the order of the spans is crucial when evaluating system performance.

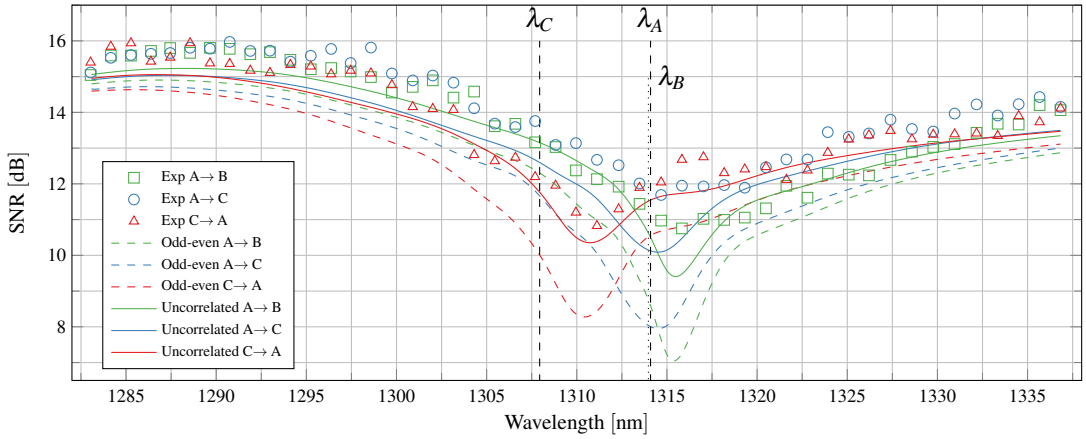

Fig. 4: After two span transmission the SNR of the central channel at a fixed per channel launch power of +6 dBm for different span orders. Coloured lines showing the SNR from simulations, dashed for odd-even and solid for uncorrelated channels. Vertical dashed lines showing the zero dispersion wavelengths of Span A, B and C

The dashed lines show simulations for the odd-even configuration and solid line for three uncorrelated channels. The uncorrelated scheme is a more realistic situation where each channel contains independent data. When there was correlation in the adjacent channels the NLIN at the peak wavelengths was 2.4, 2.1 and 2.1 dB for A→B, A→C and C→A, respectively. The severe impact of odd channel correlation was not seen in the experimental data; as the odd channels used two independent laser sources which were not perfectly phasematched, with a linewidth of <200 kHz, unlike in the simulations, where the laser phase noise was not included. This may have mitigated the buildup of NLIN.

As each span was connectorised [3], the zero dispersion wavelength for each span was measured in 15 km sections. The results for Span C were 1307.1, 1307.5 and 1309.7 nm in transmission order. All the other spans had zero dispersion wavelengths within 0.3 nm of the average shown in Fig. 2a. As the zero dispersion wavelength was found to vary within a span, this would further increase the complexity of the NLIN generation within a span. This may explain why the experimental results do not show as much peak NLIN generation as the simulations. Although more wavelengths are potentially affected, the maximum amount of NLIN is lower. This means for future O-band transmission systems be awake of the fibre's characteristics, or new standardisation is required for specifying zero dispersion wavelengths.

4. Conclusion

We have demonstrated that for coherent transmission in O-band, nonlinear interference noise, most likely from four wave mixing, is strongly dependent on the zero dispersion wavelength. As the noise generation process is nonlinear, the order of the spans is important and affects the amount and spectral width of noise. Although all fibres were G.657.A1 compliant the variation in zero dispersion wavelength within a span is also key knowledge to predict transmission performance.

Acknowledgements

A part of this research was supported by NICT/No.20301, Japan, UK EPSRC TRANSNET Programme Grant EP/R035342/1 and Microsoft 'Optics for the Cloud' Alliance. The authors thank Dr. Vitaly Mikhailov (OFS Laboratories) for the loan of BDFAs

References

1. D. Tauber *et al.*, "Role of coherent systems in the next DCI generation," *J. Light. Technol.*, vol. 41, no. 4, pp. 1139–1151, 2023.
2. https://www.oiforum.com/technical-work/hot-topics/800g-coherent/.
3. Y. Wakayama *et al.*, "400GBASE-LR4 and 400GBASE-LR8 transmission reach maximization using bismuth-doped fiber amplifiers," *J. Light. Technol.*, vol. 41, pp. 3908–3915, June 2023.
4. D. J. Elson *et al.*, "9.6-THz single fibre amplifier O-band coherent DWDM transmission," in *OFC 2023*. Th4B.4.
5. V. Mikhailov *et al.*, "Amplified transmission beyond C- and L- bands: Bismuth doped fiber amplifier for O-band transmission," *J. Light. Technol.*, vol. 40, pp. 3255–3262, May 2022.
6. D. J. Elson *et al.*, "115.2-thz aggregate bandwidth O-band coherent DWDM transmission over high-density 250-μm coating multicore fibre," in *ECOC 2023*. Th.C.2.3.
7. F. Forghieri *et al.*, "Reduction of four-wave mixing crosstalk in wdm systems using unequally spaced channels," *IEEE Photonics Technology Letters*, vol. 6, no. 6, pp. 754–756, 1994.
8. O. Sinkin *et al.*, "Optimization of the split-step fourier method in modeling optical-fiber communications systems," *J. Light. Technol.*, vol. 21, no. 1, pp. 61–68, 2003.
9. P. Poggiolini *et al.*, "Closed form expressions of the nonlinear interference for UWB systems," in *ECOC 2022*. Tu1D.1.
10. K. Inoue, "Four-wave mixing in an optical fiber in the zero-dispersion wavelength region," *J. Light. Technol.*, vol. 10, no. 11, pp. 1553–1561, 1992.
11. G. A. Sefler, "Frequency comb generation by four-wave mixing and the role of fiber dispersion," *J. Light. Technol.*, vol. 16, no. 9, p. 1596, 1998.